CREEP SOFTENING AND STRENGTHENING MECHANISMS DUE TO γ' RAFT DEVELOPMENT IN SMP 14 SINGLE CRYSTAL NICKEL BASE SUPERALLOY AT 1000 ℃

MAURIZIO MALDINI*, VALENTINO LUPINC, GIULIANO ANGELLA

The high temperature mechanical behaviour of nickel base superalloys depends mainly on the reinforcing γ' precipitate volume fraction and on its morphology that evolves significantly during deformation particularly at high temperature. In single crystal nickel base superalloys characterised by negative misfit between γ' and the γ phases, the original cuboidal γ' microstructure develops into a lamellar γ/γ' pattern perpendicular to the loading axis, when the alloys are crept at high temperature under tensile load along a $\langle 001 \rangle$ crystallographic direction.

The typical creep curves of nickel base superalloys are characterised by three or four different creep stages. Such stages can be rationalised in terms of evolution of the reinforcing γ' phase morphology during creep. The aim of this paper is to investigate the effects of γ' morphology evolution on the long tertiary creep behaviour of the nickel base superalloy SMP 14 at 1000 ℃.

K e y w o r d s: creep, single crystal nickel base superalloy, microstructure

MECHANIZMY CREEPOVÉHO ZMÄKČOVANIA A SPEVŇOVANIA SPÔSOBENÉ VÝVOJOM „RAFTOV“ γ' V MONOKRYŠTALICKEJ NIKLOVEJ SUPERZLIATINE PRI 1000 ℃

Vysokoteplotné mechanické vlastnosti niklových superzliatin závisia predovšetkým od objemového podielu spevňujúcich precipitátov γ' a od ich morfológie, ktorá sa významne mení najmä v priebehu deformácie pri vysokých teplotách. V monokryštalických niklových superzliatinách, ktoré sú charakteristické negatívnym rozdielom mriežkových parametrov medzi fázami γ' a γ, pôvodne kubická mikroštruktúra γ' sa mení na lamelárnu γ/γ'. V prípade creepu pri vysokej teplote, ako aj pri ťahovom zaťažení v smere rovnobežnom s kryštalografickým smerom $\langle 001 \rangle$ sú lamely orientované kolmo na os zaťaženia.

CNR – IENI, Consiglio Nazionale delle Ricerche – Istituto per l'Energetica e per le Interfasi, Via Cozzi 53, 20125 – Milan, Italy

* corresponding author, e-mail: maldini@ieni.cnr.it

Typické creepové deformačné krivky niklových superzliatin sa vyznačujú tromi alebo štyrmi štádiami. Tieto štádiá je možné objasniť vývojom morfológie spevňujúcej fázy γ' počas creepu. Cieľom príspevku je skúmať vplyv zmeny morfológie γ' na dlhodobé creepové vlastnosti niklovej superzliatiny SMP 14 pri teplote 1000 °C.

1. Introduction

For temperatures/stresses that are relevant for the service, the creep curve shapes of γ' reinforced nickel base superalloys are generally characterised by a large and dominant tertiary stage after a small and short decelerating primary creep, whilst usually no steady state creep rates are observed. The accelerated tertiary creep can be properly described by a linear dependence of strain rate on strain [1–3] as follows:

$$\mathrm{d}\varepsilon/\mathrm{d}t = (\mathrm{d}\varepsilon/\mathrm{d}t)^{\circ}(1 + C\varepsilon), \tag{1}$$

where $\mathrm{d}\varepsilon/\mathrm{d}t$ and ε correspond to the instantaneous strain rate and the strain, respectively, C is a parameter and $(\mathrm{d}\varepsilon/\mathrm{d}t)^{\circ}$ represents the extrapolated tertiary creep strain rate at $\varepsilon = 0$ and corresponds to the minimum creep rate if the primary creep mechanisms are not active. The relationship (1) has been physically justified in [4] supposing that the softening in nickel base superalloys is due to the accumulation of mobile dislocations whose density is proportional to the creep strain. Time softening due to the particle ripening, has been considered to have only a secondary effect on the creep curves essentially because particle size sensitive mechanisms can be activated only at high stress and in short creep tests, when just slight growth of particles can take place. At low stresses, during long-term creep tests, the particle size can strongly increase, but the creep mechanisms are only slightly sensitive to particle size. This has been clearly demonstrated by Tipler and Peck who found that a prior ageing the conventionally cast alloy IN738LC produces a decrement of the creep life at high stresses, but it has practically no effect for tests at low stresses, typical of the service conditions [5]. The small importance of the thermally induced softening, or, in general, of the reinforcing particle instability on the creep curve shape, has been taken for granted also for single crystal superalloys and the long tertiary creep has been attributed mainly to the strain softening and described by Dyson and McLean [1]. Modern single crystal nickel base superalloys show a kind of microstructure instability that can occur only to a limited extent in conventionally cast Ni base superalloys. In particular, single crystal nickel base superalloys characterised by negative misfit between γ' and the γ phases, with a large fraction of hardening cuboidal γ', if creep-tested under tensile load along a $\langle 001 \rangle$ crystalline direction at high temperature, can produce a lamellar or rafted γ/γ' pattern perpendicular to the loading axis. Neglecting the microstructure instability, under those circumstances, can be an oversimplification since the raft development can strongly influence the dislocation mobility, particularly at low stresses when the dislocations cannot easily cut the long rafted γ'.

The present paper shows the influence of the γ' morphology evolution on the creep strain rate of SMP 14 superalloy at 1000 ℃. A better knowledge of the influence of the γ' morphology evolution on the creep curve is useful both for developing new alloys to be utilised in single crystal components and to improve methodologies able to predict service life of heavily loaded components, ensuring their more efficient use.

2. Material and experimental procedures

Fully heat-treated 12 mm diameter bars of SMP 14 single crystal alloy have been supplied by Ross & Catherall Ltd, Sheffield, UK. The alloy was developed by CSIR, Pretoria, Republic of South Africa. Deviations of ⟨001⟩ crystalline direction from the rod axis were within 6°. The nominal composition of the alloy is reported in Table 1.

Table 1. SMP 14 chemical composition [wt.%]

Cr	Co	Mo	W	Re	Ta	Al	Nb	Ni
4.8	8.1	1.0	7.6	3.9	7.2	5.4	1.4	bal

The SMP 14 heat treatment consisted in complete solutioning of the alloy by a six-stage heat treatment up to the maximum temperature of 1308 ℃ followed by 16 h/1080 ℃ + 16 h/870 ℃. As a result of such heat treatment the mean size of the cuboidal intermetallic γ' phase imbedded in the γ matrix was 0.45 μm and the γ' hardening phase occupied approximately 2/3 of the alloy volume. A wider microstructure characterisation and a mechanical comparison with CMSX-4 can be found in [6]. Some material was subject to a further overage heat treatment (300 h/1050 ℃ + 100 h/1000 ℃) before being creep tested in order to study the effect of coarsened microstructure on the creep behaviour.

The constant load creep tests were performed in air with test pieces machined from directionally solidified rods. Strain was measured on 28 mm gauge length and 5.6 mm gauge diameter specimens, using capacitive transducers connected to extensometers that were clamped to the shoulders of the specimen. Three thermocouples were placed in the gauge length to control and monitor temperature gradients during creep. Before starting each test, cold (room temperature) and hot (testing temperature) partial loading was performed in order to obtain the value of the superalloy elastic modulus, and to check the absence of any bending in the specimens.

In order to study the evolution of the γ' microstructure and in particular the raft development, interrupted creep tests have been run. Microstructure micrographs were obtained by scanning electron microscopy (SEM) from random section

taken along planes parallel to the tensile stress axis. The surfaces were mechanically polished and etched with 3 HCL + 1 HNO_3 + 3 Glycerine at $\sim 0\,^{\circ}C$. The observation of the microstructure in the crept specimens outside of the gauge length, where the stress was 10 % lower compared to the applied stress on the gauge section, but the temperature was the same, has allowed widening the time-stress-temperature range conditions for the observation of raft formation.

3. Experimental creep results

In this paper the results from creep tests to rupture and interrupted creep tests on SMP 14 at 1000 °C in the nominal applied stress range from 175 to 230 MPa are reported. The creep test conditions produced in the superalloy times to rupture between 270 and 1200 h. The results are summarised in Table 2 whereas in Fig. 1 the experimental data curves describing the SMP 14 creep behaviour are reported.

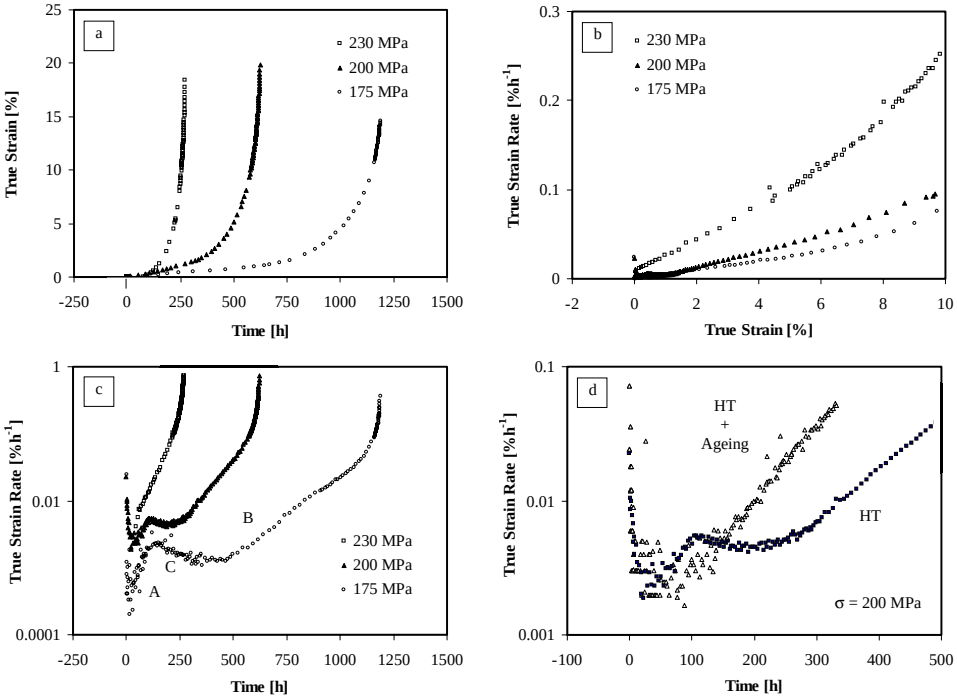

Fig. 1. Constant load and temperature experimental creep curves at 1000 °C and different applied engineering stresses: a) strain vs. time, b) strain rate vs. strain, c) log (strain rate) vs. time, and d) log (strain rate) vs. time of over-aged material (300 h/1050 °C + 100 h/1000 °C) compared with the conventionally heat-treated material.

Table 2. Experimental creep results of SMP 14 alloy

Temperature [°C]	Stress [MPa]	Time to rupture [h]	Elongation to fracture [%]	Reduction of area [%]
1000	230	276.6	22.0	29.4
	200	622.9	21.6	28.7
	200*	330*		
	200**	330**	4.5**	
	175	1188.7	17.4	30.9

* Interrupted test
** Interrupted test of conventionally heat treated + 300 h/1050 °C + 100 h/1000 °C

Fig. 1a shows the creep curve, ε vs. time, whilst $\mathrm{d}\varepsilon/\mathrm{d}t$ vs. ε and $\log(\mathrm{d}\varepsilon/\mathrm{d}t)$ vs. time curves are presented in Figs. 1b,c, respectively. In Fig. 1d the creep curves in $\log(\mathrm{d}\varepsilon/\mathrm{d}t)$ vs. time format from conventionally heat-treated (HT) and aged (HT + Ageing) SMP 14 creep tests at 1000 °C and 200 MPa are reported.

In Fig. 1a the creep curve shows that the tertiary creep dominated the creep curves. These results are consistent with those obtained for other single crystal nickel base superalloys [2, 7]. After the initial loading a conventional primary creep, where the strain rate decreases from an initially high value, has been found in the tests at 1000 °C. However, although the importance of the primary creep tends to increase with the applied load, its contribution to the total creep strain is always very small. Figs. 1a,b reveal that the small decelerating/primary stage is not followed by a steady state and only a minimum creep rate could be detected. Furthermore the experimental data presented in Fig. 1b show that Eq. (1) can well describe the experimental rate of strain accumulation up to almost the whole experimental tertiary creep in terms of time, considering the increasing stress during constant load creep. It is noteworthy that the plots in Figs. 1b,c are equivalent (although the curves appear very different), since experimental points that show a linear relationship in a plot $\mathrm{d}\varepsilon/\mathrm{d}t$ vs. ε, display a linear relationship also in a plot $\log(\mathrm{d}\varepsilon/\mathrm{d}t)$ vs. time. However, the usefulness of presenting the creep data in $\log(\mathrm{d}\varepsilon/\mathrm{d}t)$ vs. time format, rather than $\mathrm{d}\varepsilon/\mathrm{d}t$ vs. ε, is due to the capability of the plot $\log(\mathrm{d}\varepsilon/\mathrm{d}t)$ vs. time of expanding the initial portion of the creep curve, where little strain is accumulated in a relatively long time. In such a way the details that could not be evident in the conventional creep curves or in the $\mathrm{d}\varepsilon/\mathrm{d}t$ vs. ε plots, but that could be determinant in detecting time dependent effects in the material, can be observed. The comparison of the same creep curves reported in a plot $\log(\mathrm{d}\varepsilon/\mathrm{d}t)$ vs. time (Fig. 1c) clearly reveals new unusual features that are hidden in the $(\mathrm{d}\varepsilon/\mathrm{d}t)$ vs. ε plots (Fig. 1b). The experimental results show a significant dependence of creep curve shape on applied stress, which can be outlined in the following points:

– at the highest stress, a single straight line can approximate the tertiary creep along most of the specimen creep life. In the last portion of creep curve, fracture mechanisms produce a further increment of creep strain rate against the time leading to final fracture;

– at lower stresses the dominant tertiary creep comes into three different rate stages of damage accumulation before fracture mechanisms start influencing the creep curves, labelled A, C, and B in Fig. 1c.

During the first accelerated creep stage, labelled A, and starting after the minimum creep rate, about 1 % of strain is accumulated. The following regime of strain accumulation, stage C is characterised by a negative slope producing a deceleration of the creep strain. The importance of such a stage decreases when the applied stress is increased disappearing at 230 MPa. After the stage C a further accelerated creep stage, B, appears having a positive slope of smaller value compared to the slope of the stage A.

It is noteworthy that the creep curve obtained with the over-aged material (HT + Ageing) did not show a three stage tertiary creep when creep tested at 200 MPa as reported for conventionally heat-treated SMP 14 (HT). However, ordinary one-stage tertiary creep behaviour was observed with a monotonically increasing strain rate (Fig. 1d).

4. Microstructure evolution during creep

In Fig. 2a the prior creep testing microstructure that resulted from the conventional heat treatment (HT) is reported. The structure is characterised by the intermetallic cuboidal γ' hardening phase embedded in the soft γ matrix. The SEM analysis of longitudinal sections of test pieces has shown that in all SMP 14 specimens that were crept to rupture the initial cuboidal γ' microstructure evolved turning into rafts. The rafted microstructure was detected both inside and outside the gauge length, where the stress was 10 % lower compared to the applied stress in the gauge section, but the temperature was the same.

Both conventionally heat-treated and an over-aged specimen were creep tested at 1000 ℃/200 MPa for 330 h. SEM observations showed that the rafted microstructure was developed in both specimens although the lamellae in the over-aged material appear definitely wider and coarser (Figs. 2b,c).

5. Discussion

The effect of the rafting on creep must be taken into account to accurately describe the creep curves, as the model proposed by Eq. (1) can adequately describe only the creep curve when the γ' microstructure can be considered stable, i.e. in the tests run at the highest applied stresses, or after the first tertiary creep, when the strain accumulation is quicker than the microstructure evolution.

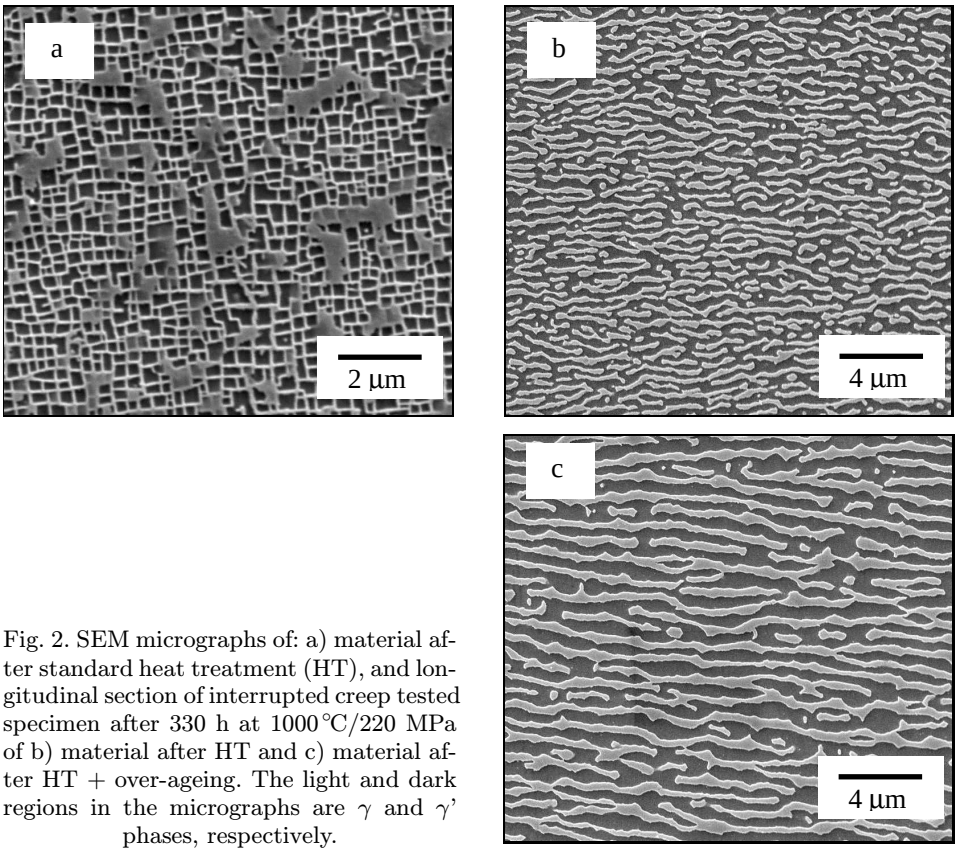

Fig. 2. SEM micrographs of: a) material after standard heat treatment (HT), and longitudinal section of interrupted creep tested specimen after 330 h at 1000 °C/220 MPa of b) material after HT and c) material after HT + over-ageing. The light and dark regions in the micrographs are γ and γ' phases, respectively.

The here-reported experimental creep results on SMP 14 alloy can be rationalised considering the dislocation difficulty both to move in the thin γ channels and to penetrate in the reinforcing γ' phase. TEM observations from different authors on different single crystal nickel base superalloys, e.g. in [8], show that during the first creep at $T \geq 850$–$900\,°C$ and stresses of interest for industrial applications, the dislocations are forced to bow in the narrow γ channels, where at first all the plastic strain takes place.

The dislocation motion is controlled by the stress in the γ phase that exceeds the Orowan resistance of the γ channels and the solid solution resistance. The former strongly depends on the microstructure of the reinforcing phase, while the latter is, as a first approximation, microstructure independent, and for this reason it will not be taken into account here.

As reported in [8] the superposition of an external applied tensile stress with the coherency (misfit) stresses causes, at the beginning of the creep test, different

values of the local stresses in the γ channels oriented perpendicular and parallel to the load axis. For negative misfit alloys ($a_{\gamma'} < a_{\gamma}$, where $a_{\gamma'}$ and a_{γ} are respectively the lattice parameters of the γ' and γ), as in the alloy here investigated, the external applied tensile stress along [001] combines with the misfit stresses in the γ channels perpendicular to the stress axis, but it is, in some measure, compensated by a component of the compressive misfit stress in the γ channel parallel to [001]. As a result, a larger shear stress exists in the horizontal γ layers, perpendicular to the stress axis. The following expression for Orowan bowing threshold stress can be utilised [8]:

$$\tau = (2/3)^{0.5} \mu b/h, \tag{2}$$

where μ is the shear modulus, b is the length of the Burgers vector, h is the γ channel thickness and the numerical factor takes into account that the dislocations glide on the slip system $\{111\}\langle 110\rangle$. Taken $\mu = 35$ GPa for cuboidal γ' microstructure, $h = 80$ nm, (estimated value supposing the volume fraction of the γ' phase is 50 % at 1000 ℃) and $b = 0.254$ nm, the resolved Orowan resistance on the slip system is about $\tau = 90$ MPa, corresponding to a uniaxial stress of about 220 MPa, comparable with the applied stress utilised in this work.

Quantitative measurements of a representative Orowan threshold stress are difficult, considering that there is an initial distribution of γ' cubes and differences exist between dendritic and interdendritic regions, producing in the material a distribution of threshold stresses. More than the correct value, we want to emphasise that the threshold stress for the Orowan bowing in high γ' volume fraction superalloys is comparable to the external applied stresses. With cuboidal γ' microstructure, the misfit stresses are expected to be very important to oppose or promote the dislocation activity in vertical and horizontal γ channels, respectively, and then to determine the strain rate during the first creep.

During plastic strain, just after the initial loading, dislocations are deposited on the γ/γ' interface, reducing the coherent stresses and making more difficult for the dislocations to move. The local stress in some channels can become not sufficiently high to activate the Orowan mechanisms, producing the strain rate decrement during the initial decelerating/primary creep.

The first accelerated tertiary creep (stage A in Fig. 1c) has been ascribed to the raft development. This assumption is supported by the creep results obtained at lower and higher temperature, than here analysed, both on SMP 14 [9] and on a different superalloy [10].

Two factors can contribute to the acceleration of the strain experimentally detected during the rafted structure development (Fig. 1c):

– The building up of the raft microstructure goes with a significant increment of the thickness h of the horizontal γ channels perpendicular to the applied stress, producing a reduction of the Orowan resistance (2).

– The development of rafting produces an increment of the alloy volume that can easily be deformed. In fact, due to the misfit stress, most of the deformation happens in the horizontal γ channels, where the local stress is higher compared to the average stress in the vertical channels. When the structure is still cuboidal, only about 10 % of the alloy volume (1/3 of the γ phase) contributes to the creep strain, while all the γ volume contributes at the strain when the rafts are completely developed.

An opposite effect on the strain acceleration of the latter mechanisms can occur, when rafts are developed, since mobile dislocations inside the γ phase cannot circumvent anymore the γ' phase by glide/climb mechanisms promoting a deceleration of the strain. In fact the accumulation of plastic strain in γ phase only, where all the mobile dislocations are, provides a local redistribution of stress in the alloy: the stress is decreased in γ phase and amplified in γ' phase, as it is expected during creep in a composite material with 'soft' (γ) and 'hard' (γ') components deforming in parallel. Hence the creep behaviour is determined by the effective stress in γ phase where all the mobile dislocations are confined. While the decreasing effective stress in the γ phase approaches the Orowan stress value, the creep decelerates, producing stage C in the plots of Fig. 1c. During creep stage C, the redistribution of the stress continues and the stress in γ' phase increases with strain up to the cutting threshold stress value when stage B in Fig. 1c plots is reached. Mughrabi et al. [11], studying the single crystal superalloy SRR 99 at 900 ℃ and 305 MPa, have found that a γ' lattice distortion was built up during the first portion of the tertiary creep, and it remained constant until the rupture, showing there was no further redistribution of the stress occurring between the two phases during the second portion of tertiary creep. These measurements are consistent with our mechanistic hypothesis.

The effects on the creep curve of the above-sketched processes are expected to be evident at low applied stresses, tending to disappear at high stress that allows the dislocations to easily move in the vertical γ channel and/or cut the reinforcing γ' phase. The higher is the value of the applied stress, the smaller is the relative redistribution of the stress between the two phases before reaching the cutting threshold stress; the tests at low stress show an evident C stage.

Creep accelerates while rafting is in progress, but we must be cautious to conclude from that, that the raft structure is detrimental to the creep properties of single crystal nickel base superalloys.

The early raft development, preventing the dislocations to circumvent the γ' phase by glide/climb and imposing the cutting mechanism, promotes a strong deceleration of the strain *after* the initial accelerated stage. From this point of view the development of the rafted structure and the consequent increment of the strain rate are the maybe inevitable penalty to pay to have a following very low strain rate and, at the end, a more creep resistant alloy.

6. Conclusions

The analysis of the experimental creep curves of the SMP14 alloy in the 175–230 MPa range at 1000 ℃ has shown that:

– The tertiary creep dominates the creep curves.

– The raft development is very rapid and takes only a few percent of the creep life.

During tertiary creep, different stages of strain rate can be observed:

– A strongly accelerated stage that occurs during the raft evolution.

– A stage that produces a reduction of the strain rate for the lowest stresses explored. This stage has been attributed to a redistribution of the local stresses between γ and γ' phases, and it disappears in the highest stress test.

– A further stage, where the strain accelerates again, with the strain rate following a linear strain softening relationship.

– The final accelerated stage with fastest strain rate leading to fracture.

Acknowledgements

The authors are grateful to Ross & Catherall Ltd, Sheffield, UK, for supplying the SMP 14 alloy rods.

REFERENCES

[1] DYSON, B. F.—MCLEAN, M.: Acta Metallurgica, *31*, 1983, p. 17.
[2] MALDINI, M.—LUPINC, V.: Scripta Metallurgica, *22*, 1988, p. 1737.
[3] MALDINI, M.—HARADA, H.—KOIZUMI, Y.—KOBAYASHI, T.—LUPINC, V.: Scripta Materialia, *43*, 2000, p. 637.
[4] DYSON, B. F.: Revue Physics Applied Letters, *23*, 1988, p. 605.
[5] TIPLER, H. R.—PECK, M. S.: NPL Report DMA A33, NPL, Teddington, UK 1981.
[6] GRAVILL, N.—BENSON, J. M.—MCCOLVIN, G.—MALDINI, M.: In: Proc. Materials for Advanced Power Engineering 1998. Eds.: Lecomte-Beckers, J. et al. Germany, Jülich, Forschungszentrum Jülich 1998, p. 1025.
[7] HENDERSON, P. J.—LINDBLOM, J.: Scripta Materialia, *37*, 1997, p. 491.
[8] POLLOCK, T. M.—ARGON, A. S.: Acta Metallurgica et Materialia, *40*, 1992, p. 1.
[9] MALDINI, M.—LUPINC, V.—LI, H.—ANGELLA, G.: In: Proc. Materials for Advanced Power Engineering 2002. Eds.: Lecomte-Beckers, J. et al. Germany, Jülich, Forschungszentrum Jülich 2002, p. 167.
[10] MALDINI, M.—HARADA, H.—KOIZUMI, Y.—KOBAYASHI, T.—OSAWA, M.—YOKOKAWA, T.—LUPINC, V.: International Journal of Materials Processing Technology, *117*, 2001.
[11] MUGHRABI, H.—BIERMANN, H.—UNGÀR, T.: In: Proc. Superalloys 1992. Eds.: Antolovich, S. et al. Warrendale, PA, USA, TMS 1992, p. 599.

Received: 22.9.2003